Gas-phase Ion Spectroscopy of Flexible and Nonflexible Nitrophenolates: Effect of Locking the Two Phenyl Units in 4’-nitro-[1,1’-biphenyl]-4-olate by a Bridging Atom

Bjarke Møller Pedersen and Steen Brøndsted Nielsen*

Department of Physics and Astronomy, Aarhus University,
DK-8000 Aarhus C, Denmark
E-mail: sbn@phys.au.dk
**Corresponding Author*

Received 11 October 2017; Accepted 21 March 2018;
Publication 02 April 2018

Abstract

Nitrophenolates (NPs) are molecular anions that can undergo charge-transfer (CT) transitions determined by the degree of electron delocalization between the phenolate oxygen (donor group) and the nitro group (acceptor). Here we have studied four different NPs: 4’-nitro-[1,1’-biphenyl]-4-olate (**1**), 7-nitro-9*H*-carbazol-2-olate (NH linker, **2**), 7-nitrodibenzo[b,d]furan-3-olate (oxygen linker, **3**), and 7-nitrodibenzo[b,d]thiophen-3-olate (sulphur linker, **4**), and recorded their electronic absorption spectra when isolated *in vacuo* to determine the effect of locking the biphenyl spacer group between the donor and acceptor on transition energies. Absorption was identified from ion dissociation (action spectroscopy) using a homebuilt setup (sector mass spectrometer combined with pulsed laser). We find that the absorption is broad in the visible region for all four NPs with significant vibronic features. The lowest energy peak is at 601 ± 4 nm, 606 ± 4 nm, 615 ± 4 nm, and 620 ± 4 nm, for **3**, **4**, **2**, and **1**, respectively. NP **1** is flexible, and its lowest energy structure is nonplanar while the other three NPs are planar according to density functional theory calculations. Hence in the case of **1** the electronic

Journal of Self-Assembly and Molecular Electronics, Vol. 6_1, 1–12.
doi: 10.13052/jsame2245-4551.6.001

transition has a higher degree of CT than for the other three, accounting for its absorption furthest to the red. Our work demonstrates that oxygen and sulphur are best at conveying the electronic coupling between the donor and acceptor sites as **3** and **4** absorb furthest to the blue (*i.e.*, the degree of CT is lowest for these two NPs). Based on the average spacing between the peaks in the vibrational progressions, coupling occurs to skeleton vibrational modes with frequencies of $649 \pm 69\,\mathrm{cm}^{-1}$ (**3**), $655 \pm 49\,\mathrm{cm}^{-1}$ (**4**), and $697 \pm 52\,\mathrm{cm}^{-1}$ (**2**).

Keywords: Intrinsic electronic absorption, charge transfer, nitrophenolates, mass spectroscopy.

1 Introduction

Hyperpolarizable organic molecules are important building blocks for optical materials [1]. One example is push-pull chromophores, *e.g.* nitrophenolates (NPs) that undergo charge-transfer (CT) transitions where electron density is transferred from the phenolate oxygen to the nitro group upon photoexcitation. However, the $\pi\pi^*$ transition is not purely CT in character as the donor and acceptor orbitals are highly delocalized and overlap somewhat. This is relevant as electronic transition energies of molecules are closely associated with the character of the electronic transition. Often, larger π-conjugation leads to lower transition energies. However, it is not always this simple if the transition changes character and becomes more CT, *e.g.*, if the symmetry [2] or planarity of a molecule is broken. Indeed, a breaking of π-conjugation between two parts (donor and acceptor) can lead to redshifted absorption. In the area of molecular electronics where single molecules are employed as electrical components, it is relevant to understand how different π-networks convey electronic coupling as for example the degree of planarity determines the conductance, which again is correlated with the transition energy [3].

Information on the intrinsic transition can be difficult to obtain from solution-phase experiments as solvent molecules can significantly alter the transition, both with regard to transition energy and character. There exists several solvent polarity scales [4–7] but extrapolation to vacuum is nontrivial for ionic chromophores due to ion-pair formation in nonpolar solvents. To obtain information on the intrinsic electronic properties of molecular ions in the absence of counter ions, it is therefore necessary to study the species isolated *in vacuo* free from any perturbing interactions. We have in a series of papers on NPs (molecular anions) demonstrated that the transition energy is low if the π-bridge only weakly conveys the electronic coupling between

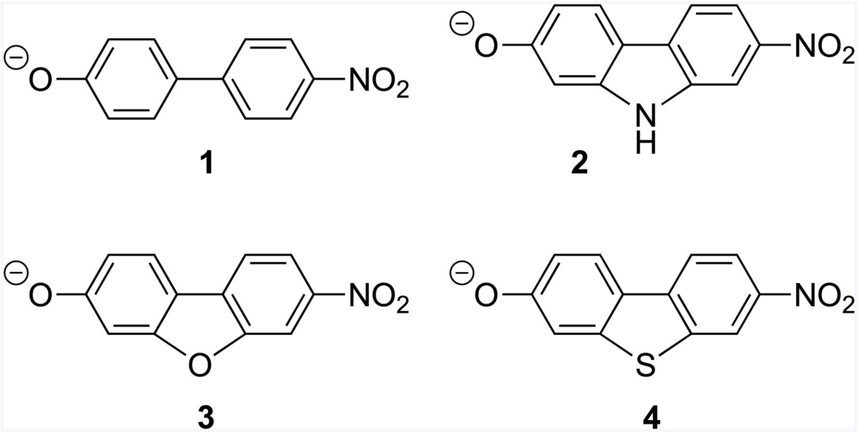

Figure 1 Chemical structures of the four nitrophenolates for study: 4'-nitro-[1,1'-biphenyl]-4-olate (**1**), 7-nitro-9*H*-carbazol-2-olate (**2**), 7-nitrodibenzo[b,d]furan-3-olate (**3**), and 7-nitrodibenzo[b,d]thiophen-3-olate (**4**).

the donor and acceptor groups [8, 9]. A single water molecule bound to the phenolate oxygen can also break the electron delocalization, causing absorption to the red of that of the bare ion [10]. This may seem counterintuitive but is simply related to the donor and acceptor orbitals coming close in energy when they are uncoupled.

In this work, we have looked at the NP where the π-bridge between the phenolate oxygen and the nitro group is biphenyl (**1**) and NPs where the two phenyl units in biphenyl are locked via a bridge atom (NH (**2**), O (**3**), or S (**4**)) (see Figure 1). Locking the two rings increases the overlap of the π-orbitals (larger π-conjugation) but decreases thereby the degree of CT. To identify the overall effect on transition energies, we have recorded electronic absorption spectra of the bare ions isolated *in vacuo* and demonstrate that the linker effect indeed represents a fine-tuning of the degree of CT character.

2 Experimental Procedures

2.1 Gas-phase Ion Spectroscopy

Experiments were done at a homebuilt setup that has already been described [11, 12]. Ions produced by electrospray of samples dissolved in methanol were stored in an octopole ion trap for 25 ms. They were then all accelerated to 50-keV energies (singly charged ions), and those of interest were selected by an electromagnet. Every second ion bunch was irradiated with visible light from 20-Hz pulsed laser system (EKSPLA). The 1064-nm output from a Nd:YAG laser was frequency tripled to 355 nm. The UV light was sent into an optical parametric oscillator (OPO) to generate the visible and idler outputs. Ion dissociation was identified from a second mass-analysis stage using a hemispherical electrostatic analyzer. A channeltron was used to detect the fragment ions. The photoinduced signal was obtained from the difference between 'laser-on' and 'laser-off' signals.

2.2 Synthesis

Nitrophenolates were synthesized as the phenols by the group of Prof. M. Brøndsted Nielsen (University of Copenhagen); the protocols are already reported in the literature [13].

3 Computational Procedures

Geometric structures of the four NPs were optimized at the B3LYP/6-31+G(d) level of theory using the Gaussian03 program package [14]. Vibrational frequencies were calculated to verify that the obtained structures are minima on the potential energy surface and not transition states.

4 Results

A representative PID mass spectrum of **2** is shown in Figure 2 obtained with an excitation wavelength of 570 nm. There are four main dissociation channels that are ascribed to the loss of either NO or NO_2 or the formation of CN^- or $NO_2{}^-$. Similar fragmentation was seen for the other three ions though the yield of CN^- and $NO_2{}^-$ was tiny in the case of **4**.

In our experiment dissociation of the mass-selected ions is monitored on the microsecond time scale, the time from photoexcitation until the ions reach the electrostatic analyzer. The total time window is about 10 μs. This implies that if the time constant for dissociation is much longer than this, we will not detect much dissociation even though the ions are photoexcited. The rate constant for dissociation depends on the activation barrier, the excess energy after photoexcitation, and a frequency factor (*cf.*, a simple Arrhenius expression). Often more than one photon is needed to bring the dissociation time constants into the instrumental time window. It is therefore important to determine how many photons are required for each of the

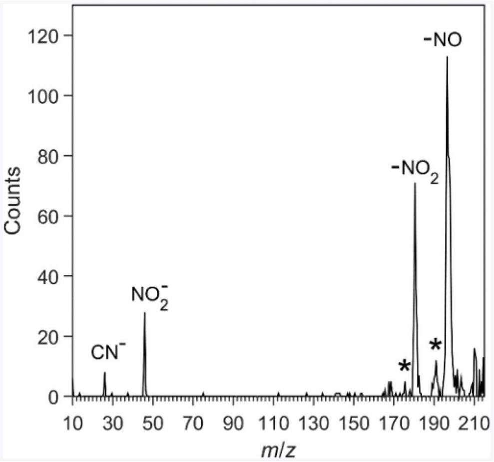

Figure 2 Photoinduced dissociation mass spectrum of **2** (excitation wavelength 570 nm). The stars label artefact peaks that are ascribed to scattering inside the analyzer (these occur at well-known positions).

Table 1 Summary of number of photons that causes dissociation on the instrumental time scale

Parent Ion	NO Loss	NO_2 Loss	$NO_2{}^-$	CN^-
1	2.0 ± 0.2	2.1 ± 0.4	2.4 ± 0.3	–
2	2.1 ± 0.3	2.1 ± 0.5	1.9 ± 0.3	2.7 ± 0.2
3	2.0 ± 0.4	2.5 ± 0.1	2.3 ± 1.0	–
4	2.1 ± 0.3	2.5 ± 0.8	–	–

dissociation channels. This information is simply obtained from the yield of a fragment ion *versus* laser power (*i.e.*, number of photons in the laser pulse). The results are summarized in Table 1. It is evident that two photons are needed for most of the channels, in the case of CN^- formation two to three photons. Hence the yield of a daughter ion is related to the absorption cross section of the parent ions multiplied by the number of photons raised to the power of two or three.

Figure 3 shows the action spectra (‘laser on’ – ‘laser off’ signals, not corrected for variations in laser power at each wavelength) for the relevant fragmentation channels for each of the four ions. These spectra were obtained at full laser power to establish the relevant regions over which absorption occurs; it implies, however, that the band is saturated where absorption is high. It is clearly seen that absorption covers a broad region extending over

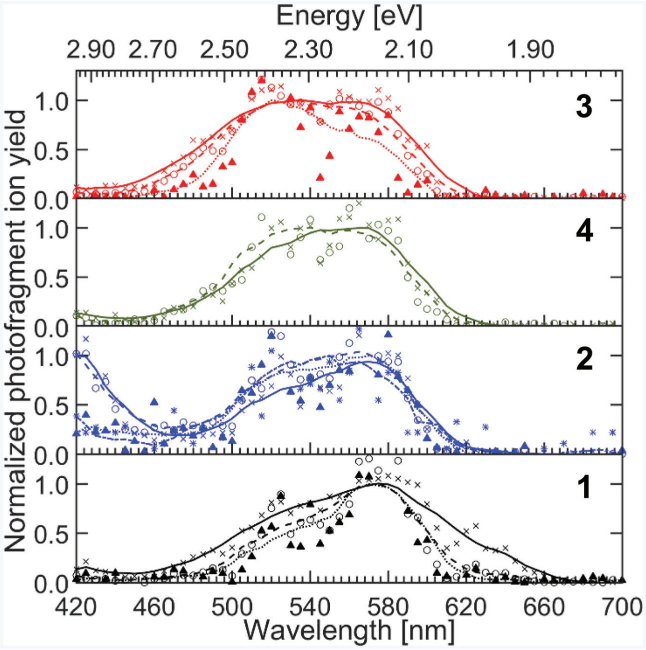

Figure 3 Action spectra of **1**, **2**, **3**, and **4**, sampling different fragment ions. The laser power was high causing saturation of the signal at band maxima. Points associated with loss of NO are indicated by ×; loss of NO_2 by o; formation of NO_2^- by Δ; and formation of CN^- by $*$.

more than 100 nm for each ion, and that the absorption by **1** is more to the red than that of the other three ions.

To avoid saturation, spectra for NO loss were recorded at a lower laser power (reduced by 60% from maximum), and the difference signal was divided by the number of photons at each wavelength raised to the power of two (according to the power dependence measurements) (Figure 4). The obtained cross section is taken to represent the absorption by the ions. We note that such an indirect approach is necessary when it comes to gas-phase ion spectroscopy as the ion density is too low to allow for traditional transmission experiments. A vibrational progression is clearly observed in the spectra of **2**, **3**, and **4**; peak maxima are summarized in Table 2. The absorption spectrum of **1** was earlier reported [9], and while the region where absorption occurred is the same as here, the shape of the spectrum is different to the one obtained in the present work. This is likely associated with issues of properly correcting for the photon dependence at each wavelength, and we therefore limit our main discussion

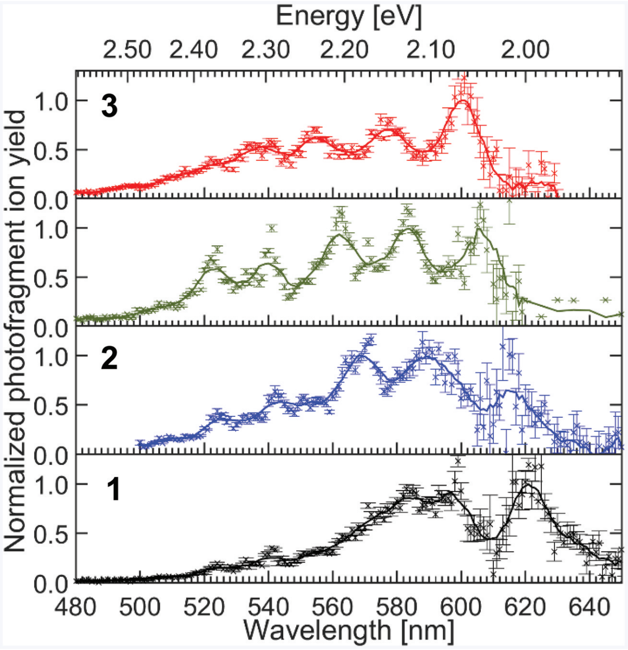

Figure 4 Action spectra of **1**, **2**, **3**, and **4** obtained at lower laser power than in Figure 3 and corrected for the number of photons at each wavelength.

Table 2 Summary of peak maxima (uncertainty ±4 nm) and band maxima in methanol solution (last column)

1	–	–	–	–	620	406
2	525	543	569	589	615	443
3	–	538	554	577	601	421
4	523	541	562	583	606	421

to the peak associated with the lowest energy transition and not to differences in band shape between the four ions. We find again that the lowest energy transition occurs for **1**, and that the transition energy increases in the order: **1** < **2** < **4** < **3**. From the separation between the peaks in each spectrum we obtain average frequencies for the modes that couple to the electronic transition; these are about 649 ± 69 cm^{-1} (**3**), 655 ± 49 cm^{-1} (**4**), and 697 ± 52 cm^{-1} (**2**) and correspond to skeleton modes. The vibronic structure is most evident in the rigid molecules, not surprisingly.

Calculated structures of the four NPs are shown in Figure 5. The geometries of **2**, **3**, and **4** are all planar while that of **1** is nonplanar with a twist angle between the two phenyl groups of 14°, in agreement with earlier density

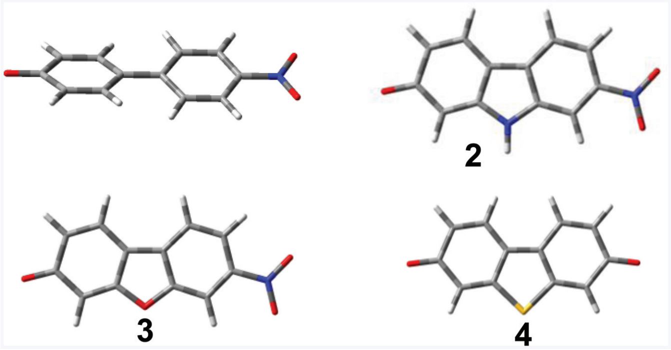

Figure 5 Calculated structures of the four NPs. Structure **1** is nonplanar in contrast to the other three that are all planar.

functional calculations [4]. MP2 perturbation theory predicts the angle to be even larger (20–29°) [9].

5 Discussion

There is a simple explanation for the blueshift seen for **2**, **3**, and **4** relative to **1**: The planarity of the three molecules together with the sp^2-hybridized bridge-atom increases the electronic coupling between donor and acceptor ends, and as a result lowers the degree of CT character. It is evident that the coupling is stronger when the bridging linker is O than when it is S or NH. The difference in absorption between **3** and **4** is small (5 nm). For comparison, the two ions have maximum absorption in methanol solution at the same wavelength (421 nm) [13]. NP **2** displays redshifted absorption compared to **3** and **4**, both in gas phase and in solution (443 nm is absorption maximum in methanol solution [13]). The difference in absorption between the three locked NPs indicates that the identity of the bridge atom does play a role, either because of differences in the overlap of its sp^2 orbital with the biphenyl sp^2 orbitals or because the N, O, and S cause slightly different geometries of the two phenyl groups relative to each other. The absorption in solution is strongly blueshifted compared to gas phase, which is in agreement with the transition having significant CT character. Indeed, as electron density moves away from the negatively charged phenolate end and towards the nitro group end upon photo-excitation, the favorable interaction with the methanol molecules that hydrogen bond to the phenolate oxygen is reduced. This may also explain why the solvent shift is largest for **1** that has the highest degree of CT, and that

1 actually absorbs further to the blue than the three other ions in methanol solution (in contrast to the situation in gas phase).

Acknowledgments

We acknowledge Dr. Tue H. Jepsen and Prof. Mogens Brøndsted Nielsen for providing the samples used in this work.

References

[1] M. J. Cho, D. H. Choi, P. A. Sullivan, A. J. P. Akelaitis, L. R. Dalton, *Prog. Polym. Sci.*, **33**, 1013–1058 (2008).
[2] I. Alata, C. Dedonder, M. Broquier, E. Marceca, C. Jouvet, *J. Am. Chem. Soc.*, **132**, 17483–17489 (2010).
[3] D. Vonlanthen, A. Mishchenko, M. Elbing, M. Neuburger, T. Wandlowski, M. Mayor, *Angew. Chem. Int. Ed.*, **48**, 8886–8890 (2009).
[4] a) K. Dimroth, A. Schweig, C. Reichardt, *Justus Liebigs Ann. Chem.*, **669**, 95–105 (1963); b) C. Reichardt, *Chem. Rev.*, **94**, 2319–2358 (1994).
[5] E. M. Kosower, *J. Am. Chem. Soc.*, **80**, 3253–3260 (1958).
[6] M. J. Kamlet, J. L. Abboud, R. W. Taft, *J. Am. Chem. Soc.*, **99**, 6027–6038 (1977).
[7] a) M. J. Kamlet, R. W. Taft, *J. Am. Chem. Soc.*, **98**, 377–383 (1976); b) R. W. Taft, M. J. Kamlet, *J. Am. Chem. Soc.*, **98**, 2886–2894 (1976).
[8] S. Brøndsted Nielsen, M. Brøndsted Nielsen, A. Rubio, *Acc. Chem. Res.*, **47**, 1417–1425 (2014).
[9] M.-B. S. Kirketerp, M. Å. Petersen, M. Wanko, L. A. E. Leal, H. Zettergren, F. M. Raymo, A. Rubio, M. Brøndsted Nielsen, S. Brøndsted Nielsen, *Chem. Phys. Chem.*, **10**, 1207–1209 (2009).
[10] J. Houmøller, M. Wanko, A. Rubio, S. Brøndsted Nielsen, *J. Phys. Chem. A*, **119**, 11498–11503 (2015).
[11] K. Støchkel, B. F. Milne, S. Brøndsted Nielsen, *J. Phys. Chem. A*, **115**, 2155–2159 (2011).
[12] J. A. Wyer, S. Brøndsted Nielsen, *Angew. Chem. Int. Ed.*, **51**, 10256–10260 (2012).
[13] T. H. Jepsen, M. Jørgensen, M. B. Nielsen, *Synthesis*, **45**, 1115–1120 (2013).
[14] Gaussian 03, Revision D.01, M. J. Frisch, G. W. Trucks, H. B. Schlegel, G. E. Scuseria, M. A. Robb, J. R. Cheeseman, J. A. Montgomery, Jr.,

T. Vreven, K. N. Kudin, J. C. Burant, J. M. Millam, S. S. Iyengar, J. Tomasi, V. Barone, B. Mennucci, M. Cossi, G. Scalmani, N. Rega, G. A. Petersson, H. Nakatsuji, M. Hada, M. Ehara, K. Toyota, R. Fukuda, J. Hasegawa, M. Ishida, T. Nakajima, Y. Honda, O. Kitao, H. Nakai, M. Klene, X. Li, J. E. Knox, H. P. Hratchian, J. B. Cross, V. Bakken, C. Adamo, J. Jaramillo, R. Gomperts, R. E. Stratmann, O. Yazyev, A. J. Austin, R. Cammi, C. Pomelli, J. W. Ochterski, P. Y. Ayala, K. Morokuma, G. A. Voth, P. Salvador, J. J. Dannenberg, V. G. Zakrzewski, S. Dapprich, A. D. Daniels, M. C. Strain, O. Farkas, D. K. Malick, A. D. Rabuck, K. Raghavachari, J. B. Foresman, J. V. Ortiz, Q. Cui, A. G. Baboul, S. Clifford, J. Cioslowski, B. B. Stefanov, G. Liu, A. Liashenko, P. Piskorz, I. Komaromi, R. L. Martin, D. J. Fox, T. Keith, M. A. Al-Laham, C. Y. Peng, A. Nanayakkara, M. Challacombe, P. M. W. Gill, B. Johnson, W. Chen, M. W. Wong, C. Gonzalez and J. A. Pople, Gaussian, Inc., Wallingford CT, 2004.

Biographies

Bjarke Møller Pedersen received his Master's degree in Physics from Aarhus University in 2016 and has since then been employed as a high school teacher at Viborg Katedralskole (Denmark).

Steen Brøndsted Nielsen earned his PhD in Chemistry in 2000 from the University of Copenhagen. During his studies, he spent time at Yale, University of Oslo and University of Alberta. He was a post doc at Aarhus University (AU) and at Princeton. He has had guest Professorships in Orsay, Caen and Villetaneuse, and been a JILA Visiting Fellow. Since 2007 he has been employed as an Associate Professor at AU. He has done research within the fields of ligated metal ions, vibrational spectroscopy of anions, protein folding dynamics, biochromophore spectroscopy, and electron induced dissociation of ions.